Neutrino Detectors: Challenges and Opportunities

F.J.P. Soler

School of Physics and Astronomy, University of Glasgow, Glasgow G12 8QQ, U.K.

Abstract. This paper covers possible detector options suitable at future neutrino facilities, such as Neutrino Factories, Super Beams and Beta Beams. The Magnetised Iron Neutrino Detector (MIND), which is the baseline detector at a Neutrino Factory, will be described and a new analysis which improves the efficiency of this detector at low energies will be shown. Other detectors covered include the Totally Active Scintillating Detectors (TASD), particularly relevant for a low energy Neutrino Factory, emulsion detectors for tau detection, liquid argon detectors and megaton scale water Cherenkov detectors. Finally the requirements of near detectors for long-baseline neutrino experiments will be demonstrated.

Keywords: Detectors; Neutrino Factories; Super Beams; Beta Beams; MIND; TASD; Liquid Argon; Water Cherenkov
PACS: 14.60.Ef,14.60.Pq,29.20.D-,29.40.-n,29.40.Gx,29.40.Ka,29.40.Mc

1. INTRODUCTION

The neutrino detectors currently being designed for the next generation of neutrino oscillation experiments at future neutrino facilities offer significant challenges in their design, construction, technology and scale. However, these detector options benefit from many advances in new technologies over the past decade, offering significant opportunities in realising these very demanding designs, which offer unprecedented accuracy in neutrino experiments and the potential to make important scientific discoveries.

This review covers possible detector options, suitable at future neutrino facilities, such as Neutrino Factories from the decay of muons, Super Beams (4 MW scale conventional neutrino beams from pion decay) and Beta Beams (from the decay of radioactive ions). Section 2 will describe the Magnetised Iron Neutrino Detector (MIND), which is the baseline detector at a Neutrino Factory, including a general description of the detector, the latest analysis which improves the efficiency of this detector at low energies, R&D challenges needed to be able to build a MIND and, finally, a brief description of the Indian Neutrino Observatory, which could be the first MIND. Section 3 will cover the Totally Active Scintillating Detectors (TASD) as an alternative to MIND, section 4 will describe emulsion detectors for tau detection, section 5 describes the R&D being carried out to build large scale liquid argon detectors, section 6 includes ideas for Megaton scale water Cherenkov detectors and section 7 includes the parameters required by near detectors for long-baseline neutrino experiments.

2. MAGNETISED IRON NEUTRINO DETECTOR (MIND)

The Neutrino Factory contains two neutrino flavours (ν_μ and $\overline{\nu}_e$ from the decay of μ^- or $\overline{\nu}_\mu$ and ν_e from the decay of μ^+). For this reason, the golden channel signature at a Neutrino Factory is the appearance of "wrong-sign" muons (from $\overline{\nu}_e \to \overline{\nu}_\mu$ or $\nu_e \to \nu_\mu$ oscillations, respectively) [1] in a magnetised detector [2]. A Magnetised Iron Neutrino Detector (MIND) between 50 and 100 kton has been shown to be the most effective way to perform a neutrino oscillation analysis to search for CP violation in the neutrino sector at a Neutrino Factory [3, 4].

2.1. MIND description

The International Design Study for a Neutrino Factory (IDS-NF) [5] and the EuroNu project [6] have defined a baseline detector configuration at a Neutrino Factory from 25 GeV muons consisting of a far detector of 100 kton at a distance between 2000 and 4000 km and a second detector with 50 kton mass at the magic distance of 7500 km [7], which is insensitive to CP violation. The optimum detector to search for the appearance of "wrong-sign" muons consists of modules 15×15 m^2 with 3 cm of iron and 2 cm of scintillator (1 cm scintillator for each of the x and y views), immersed in a 1 T magnetic field. About 1800 such modules can be placed one after each other (90 m) to make a 100 kton detector and 900 modules (45 m) make a 50 kton detector.

2.2. New analysis and sensitivity for MIND

In the original golden channel paper [2], the analysis was optimised for a 50 GeV Neutrino Factory for small values of θ_{13}, so the efficiency at low energy was cut severely. That analysis used fast simulations and a detector parameterisation, with no reconstruction or pattern recognition. The MIND analysis was redone for the International Scoping Study (ISS) [4] for a 25 GeV Neutrino Factory, with improved event selection to improve the efficiency at low energies, but still with a GEANT3 [8] based fast simulation, perfect pattern recognition, a parameterisation based reconstruction and still with a 1 T dipole field throughout the volume. The muon momentum was determined by range, for fully contained muons, and by curvature for scraping muons. The hadron shower parameterisation used was:

$$\left(\frac{\delta E}{E}\right)_{had} = \frac{0.55}{\sqrt{E_{had}}}, \tag{1}$$

from the MINOS CalDet testbeam [9, 10].

A recently published analysis [11] has been performed with full reconstruction using a Kalman filter [12] and full pattern recognition for muon selection. If there are more than five planes with only one hit, the track is defined as a muon, if less than five planes contain one hit then a Cellular Automaton algorithm [13, 14] is invoked to identify the hits associated to a muon. The simulation was still carried out using GEANT3 and with the LEPTO Deep Inelastic Scattering (DIS) lepton-nucleon event generator [15]. The analysis chain was carried out using likelihood functions to separate signal from background. However, the 1 T dipole field was still present and the same hadron shower smearing function (equation 1) was used. The results after the analysis show an improvement in the signal efficiency at low energies from the ISS result, even after invoking a more realistic reconstruction and pattern recognition, with backgrounds of less than 10^{-3}. Another important output was the publication of full response (migration) matrices for signal and background, that allow calculation of the sensitivity and can be used for full systematic studies.

A new analysis of the performance of MIND has been carried out [16]. Improvements were made to the MIND analysis, now with a full GEANT4 simulation [17], with the inclusion of quasi-elastic scattering and resonance production using the NUANCE event generator [18]. The inclusion of non DIS processes dominates at low energies so it improves the detection efficiency at low energies.

The smearing of hits is still performed according to the same hadronic energy resolution function (equation 1), with the digitisation of hits into squares (named "voxels") of the correct spatial resolution ($\sim$ 1 cm), which corresponds to scintillator strips of width 3.5 cm. The clustering of hits is performed using a crude digitisation algorithm. The raw deposit energy of each voxel is attenuated assuming wavelength shifting (WLS) fibres with attenuation length $\lambda = 5$ m, as reported by the MINERvA collaboration [19]. The energy is halved, for each view, and smeared according to a Gaussian with $\sigma/E = 6\%$ to represent the response of the electronics. We assume a quantum efficiency of $\sim$30% and a minimum of 4.7 photoelectrons (pe) as in MINOS [10].

Probability density functions (PDF), used to create log-likelihood ratio functions between signal and background, are calculated to carry out the analysis. The wrong-sign muon signature is taken into account by calculating a curvature error PDF $\left(\sigma_{q/p}\right)/(q/p)$, where q is the calculated charge (± 1) and p is the momentum of the candidate muon. A log-likelihood ratio function $\mathscr{L}_{q/p} > -0.5$ is used to select signal from background.

Further likelihoods used to separate signal fron neutral current background include the number of hits, the fraction of visible energy and the mean energy deposit per plane for the candidate muon. These likelihood functions were motivated by the MINOS analysis [20]. No added background rejection was achieved by using the latter two variables, probably due to correlations between variables, so this analysis was based only on the number of hits in the candidate to form the log likelihood rejection parameter:

$$\mathscr{L}_1 = \log\left(\frac{l_{hit}^{CC}}{l_{hit}^{NC}}\right) > 1.0, \tag{2}$$

where l_{hit} is the PDF for the number of hits.

A series of kinematic cuts, based on the momentum and isolation of the candidate, as related to the reconstructed neutrino energy of the event, $E_\nu = E_\mu + E_{had}$, can be used to reduce backgrounds from decays. The variable $Q_t = P_\mu \sin^2\theta$ is the muon isolation variable, with θ the angle between the muon and the hadronic jet and P_μ the momentum of the muon. The following cuts:

$$E_{rec} \leq 5 \text{ GeV or} \quad Q_t > 0.25 \text{ GeV/c} \tag{3}$$

$$E_{rec} \leq 7 \text{ GeV or} \quad P_\mu \geq 0.3 \cdot E_{rec} \tag{4}$$

are an effective way to reduce all of the relevant beam related backgrounds.

A fiducial cut, in which the vertex is 2 m from the end of the detector is also introduced. An additional set of quality cuts to reject errors in the bending radius of muons was implemented. Accepting only those events in which the candidate muon has 60% of its clusters fitted and $E_\nu < 40$ GeV reduces the background levels.

Background events tend to be concentrated at low relative displacement and low number of hits. Events are accepted should they meet the conditions described in

equations 5 and 6:

$$\frac{dispX}{dispZ} > 0.18 - 0.0026 \cdot N_h \quad (5)$$

$$dispZ > 6000\ mm \quad \text{or } P_\mu \leq 3 \cdot dispZ, \quad (6)$$

where N_h is the number of clusters in the candidate, $dispX/dispZ$ is the displacement in the bending plane in units of mm and P_μ is the muon momentum in units of MeV/c. The final cut involves fitting the candidate's projection onto the bending plane to a parabola. If the fitted charge is opposite to that found by the Kalman filter then the event is rejected.

The backgrounds from Charged Current (CC) and Neutral Current (NC) events and the signal event selection efficiency for both polarities are summarised in Figure 1. The expected level of CC and NC background is at the 10^{-4} level. The background from ν_e ($\overline{\nu}_e$) CC interactions was found to be at the 10^{-6} level. There is a net improvement in threshold from previous analyses [2, 4, 11] due to QEL and RES events. The thresholds of the newest results at between 2-3 GeV allow sensitivity to the extraction of the oscillation parameters at 4000 km distance. The difference in efficiency between the two appearance channels is due to the distribution of neutrino and antineutrino DIS events with the Bjorken y variable $y = \frac{E_\nu - E_l}{E_\nu}$, with E_l the exiting lepton energy. Neutrino interactions tend to involve a greater energy transfer to the target, while the muons from antineutrino interactions tend to have larger momentum and so are easier to identify.

An analysis of the systematic errors emanating from a number of factors was also carried out. The determination of the parameters used to form the cuts in the analysis, the error in the determination of the hadronic shower energy and direction resolution, the uncertainty in the relative proportions of the different interaction types and any assumptions in the representation of the detector and electronics were taken into account.

A 6% error in the energy scale uncertainty (as found by MINOS [10]) has little effect on the true neutrino energy efficiencies. However, the hadronic direction resolution is likely to have far greater uncertainty. A 50% increase in the angular resolution parameters introduces a difference in efficiency at the level of 1%. The relative proportions of QEL, DIS and other types of interaction in the data sample could have a significant effect on the signal efficiencies and backgrounds. Taking the binned errors on the cross-section measurements from [21, 22], a change in the QEL content in each bin changes the efficiency ε for each bin by:

$$\varepsilon = \frac{\sigma_{QEL}}{1 + \sigma_{QEL}}, \quad (7)$$

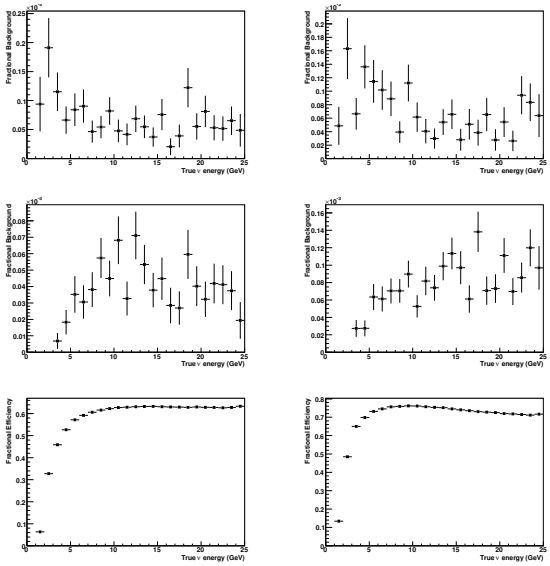

FIGURE 1. (Top-left) background from mis-identification of $\overline{\nu}_\mu$ CC reconstructed as ν_μ CC, (top-right) ν_μ CC reconstructed as $\overline{\nu}_\mu$ CC. (Middle-left) background from mis-identification of NC interactions as ν_μ CC, (middle-right) NC reconstructed as $\overline{\nu}_\mu$ CC. (Bottom-left) reconstructed ν_μ CC efficiency, (bottom-right) $\overline{\nu}_\mu$ CC efficiency.

where σ_{QEL} is the proportional error on the QEL cross-section for the bin. Errors for 1π resonant (RES) reactions are estimated at $\sim$20% below 5 GeV (as measured by the K2K near detector [23]) and at 30% above. The error due to other resonant reactions, coherent, diffractive and elastic processes was taken to be 50%. The 1σ systematic error for QEL, 1π resonance events and other non-DIS interactions were determined to be at the level of 1% in the efficiency threshold region.

The preliminary sensitivities obtained from this analysis by fitting the neutrino oscillation formulas to extract θ_{13}, the CP violating phase δ_{CP} and to determine the mass hierarchy can be seen in Figure 2.

Further opportunities in developing further this analysis include improving the digitisation algorithms and optimising the geometry of the detector to include a more realistic detector configuration (similar to MINOS), with a toroidal field, rather than a dipole field. The analysis would also benefit from improved hadronic reconstruction algorithms to reduce the energy and angular resolution. To be able to produce more accurate sensitivity plots, it is essential to include the ν_τ oscillation signal [24, 25] in the oscillation fits. For this reason, it is essential to move to the GENIE simulation [26], that includes τ decays and a large number of neutrino interactions. Finally, new sentivities, taking into account all the above effects and all systematic errors can be extracted.

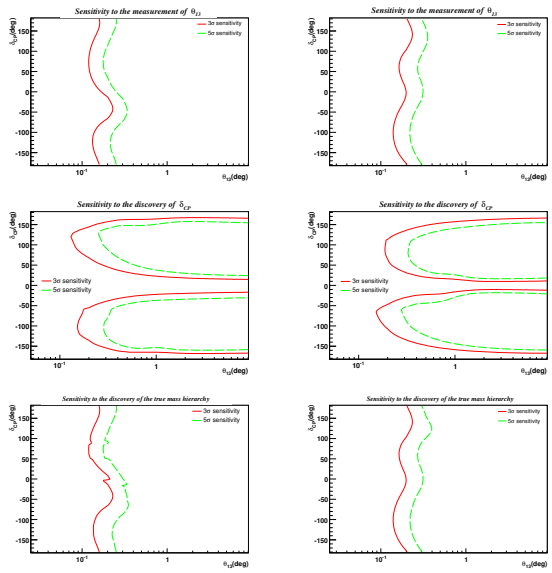

FIGURE 2. Sensitivity to θ_{13} for true normal hierarchy (top-left) and true inverted hierarchy (top-right), to δ_{CP} for true normal hierarchy (middle-left) and true inverted hierarchy (middle-right) and to the true mass hierarchy for true normal hierarchy (bottom-left) and true inverted hierarchy (bottom-right).

2.3. R&D challenges

The 1 T dipole magnetic field and plates with a rectangular geometry are not practical from an engineering point of view. A toroidal field, as in MINOS [10], is needed to avoid low B-field corners. A preliminary field map using 14 m octogonal plates from an ANSYS simulation [27] is shown in Figure 3.

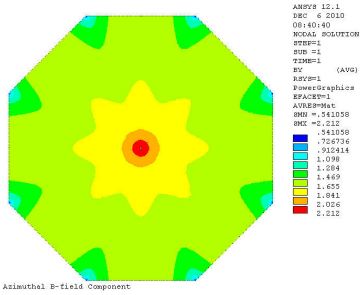

FIGURE 3. Contours of constant magnetic field in a large octogonal iron plate of 14 m height and width and 3 cm in thickness.

Fields between 1 T and 2.2 T throughout the iron plate area can be achieved with with a coil of 92 kA-turn. In MINOS, an aluminium coil with 30 cm diameter was needed to achieve 25 kA-turn [10]. A Superconducting Transmission Line (STL), a superconducting cable encompassing its own liquid helium dewar, an idea developed for the VLHC [28], could achieve 100 kA-turn with only one turn, and would only need a hole in the middle of the iron plates of 10 cm diameter.

The engineering of large 15 m plates pose significant challenges. The support of the plates is carried out by hanging them by a set of "ears". Significant stress is placed on the "ears" of the plates, but by careful engineering these can be sustained. The floor loading requires bedrock or an enormous foundation, which also needs to be taken into account.

A future R&D programme needs the construction of a prototype detector with extruded scintillator and wavelength shifting optic fibres read out by Silicon Photomultipliers (SiPM). This detector, including a realistic B-field would be used to measure and benchmark the charge misidentification rate as a function of momentum in a dedicated test beam at CERN or elsewhere, as part of the European detector R&D programme AIDA [29].

2.4. Indian Neutrino Observatory (INO)

The Indian Neutrino Observatory deserves a special mention, since it is a project that could be built in the next decade. The Iron Calorimeter of the INO is a 52 kton magnetised detector to be built in the Bodi West Hills, Madurai, India [30]. There are three modules, each of dimensions 16 m$\times$16 m$\times$14.4 m. with 5.6 cm iron plate thickness and a 1.5 T magnetic field. The tracks are read out by Resistive Plate Chambers (RPC). Its main purpose is to perform a sign selected atmospheric neutrino measurement and search for matter effects, but could be used for beam neutrinos as well, either from a Beta Beam or Neutrino Factory. The location in India is very close to the magic baseline for beam facilities in Europe and Japan (CERN to INO: 7360 km; JPARC to INO: 6570 km; RAL to INO: 7820 km), so could be the first of the MIND detectors to be built.

3. TOTALLY ACTIVE SCINTILLATING DETECTORS (TASD)

A Totally Active Scintillating Detector (TASD) inside a magnetic field has been shown to have excellent muon and electron reconstruction capabilities [4, 31]. A GEANT4 simulation of a 30 kton detector with 10,000 modules of triangular extruded scintillators, with 1,000 cells per plane, for a total of 10^7 channels immersed in a 0.5 T magnetic field was carried out. The position resolution obtained was $\sim$4.5 mm, with muon momenta reconstructed between 100 MeV/c and 15 GeV/c. The charge misidentification rate was approximately 2×10^{-5} for muon momenta greater than 400 MeV/c. The reconstruc-

tion efficiency for charged current neutrino events was found to be 98% above a neutrino energy of 500 MeV. Visual scans were carried out to estimate that the electron charge identification efficiency is $\sim 80\%$. However, automatic algorithms to develop the electron charge efficiency are still to be developed.

The charge mis-identification rate, neutrino reconstruction efficiency and neutrino energy resolution from the simulations were used to determine the physics reach of the TASD at a low energy neutrino factory [32, 33] and at a distance of 1480 km. This analysis showed that the combination of the low energy neutrino factory (5 GeV muon energy) with the low energy threshold TASD can reach a mass hierarchy and δ_{CP} sensitivity of $\sin^2 2\theta_{13} > 10^{-3}$ at 95% CL, by analysing the golden channel.

The main R&D challenge is the magnetisation of the huge volume of this detector. However, possible magnetisation can be achieved using the magnetic cavern concept, in which 10 modules with 15 m length and 15 m diameter can be magnetised using the Superconducting Transmission Line (STL) mentioned in section 2.3. A 0.58 T field with 50 kA current can be achieved, but R&D is needed to develop further the idea.

4. EMULSION DETECTORS

Emulsion detectors have a proven capability for ν_τ appearance, as in the OPERA experiment [34, 35]. The best way to identify the "silver channel" at a Neutrino Factory is using the Emulsion Cloud Chamber (ECC) concept [36]. This detector technology can be used to measure taus by searching for decay kinks and measuring the charge of particles from the tau decay. However, due to the limited statistics at a far detector facility, the optimum strategy to remove degeneracies in the neutrino oscillation formulas is by having two MIND detectors, one at 4000 km and the other at 7500 km, rather than a golden and a silver detector in the same location.

More recently, there has been interest in performing tau identification at a near detector to search for Non-Standard Interactions (NSI) [37]. However, while the tau detection efficiency of an ECC detector remains the highest, it remains to be shown how such a detector can cope with the high neutrino event rate at a near detector of a Neutrino Factory.

5. LIQUID ARGON DETECTORS

There are signficant efforts in Japan, USA and Europe to develop liquid argon detectors for current and future neutrino experiments. Neutrino interactions in liquid argon offer unprecedented level of detail, allowing for excellent identifcation and classification of neutrino events.

Liquid argon detectors operating at a neutrino beam include the T600 Icarus 600 tonne detector [38], at the Gran Sasso Laboratory (LNGS), exposed to the CERN CNGS wide band beam. This detector took cosmic ray data on the surface and is currently operating at the CNGS beam. The first neutrino events have already been recorded. The ArgoNeut detector at the NuMI beam at the Fermilab National Laboratory (FNAL) took data between May 2009 and February 2010 [39]. It has a fiducial volume of 175 l and has collected an estimated 6600 ν_μ CC interactions and 4900 $\overline{\nu}_\mu$ CC interactions.

MicroBooNE [40] is a proposal for 186 ton (70 t fiducial) to address the MiniBooNE low energy excess [41]. Furthermore, there is a proposal to install a 20-30 kton liquid argon detector at DUSEL to operate at the Long-Baseline Neutrino Experiment (LBNE) beam between Fermilab and Homestake. The aim of this detector is to perform neutrino oscillation physics but also perform a search for proton decay and search for other astrophysical signatures, such as neutrinos from supernova explosions.

There are two different approaches in Europe: one is the MODULAr project [42] and the other is the GLACIER detector [43]. MODULAr is a 20 kton proposal at LNGS, based on larger 8×8 m^2 Icarus modules, while GLACIER is a 50 to 100 kton detector based on vertical drift and read out by Large GEMs (LEMs) operating in double phase, with charge extraction and amplification in the gaseous argon phase. Significant R&D is taking place to be able to realise these concepts in large scale.

6. WATER CHERENKOV DETECTORS

The USA, Europe and Japan all have proposals for 100-500 ktonne water Cherenkov detectors, based on the very successful Super-Kamiokande design. The technology is well known from Super-Kamiokande, but the challenge is in terms of the size, cost, volume of excavation and number of photomultiplier tubes (PMT) that need to be deployed.

The LBNE water Cherenkov detector consists of two modules, each of mass 138 ktonne, with 50,000 PMTs, at the DUSEL site in the Homestake mine in South Dakota at a depth of 4850 feet [44]. The Hyperkamiokande proposal, with a water Cherenkov detector of mass 550 kton at the Kamioka site [45], or the Tokai-to-Kamioka-Korea (T2KK) proposal with two detectors each of mass 270 kton at the Kamioka mine at 295 km and a site in Korea 1100 km from the neutrino beam in Tokai [46] offer sensitivity to CP violation down to $\sin^2 2\theta_{13} > 10^{-2}$. The MEMPHYS proposal [47] aims to study neutrino oscil-

lations using a CERN beam from the Superconducting Proton LINAC (SPL) at CERN and three to five water Cherenkov detectors of total mass between 440 and 730 ktonnes at the Fréjus tunnel in France. A 30% photocathode coverage can be achived with 80,000 12 inch PMTs.

7. NEAR DETECTORS

We have learned that near detectors are essential for neutrino oscillation physics, since they are used for the measurement of the the neutrino flux, which is used to extrapolate to the far detector. In addition, these detectors are used to perform cross-section measurements in the relevant energy range (for example, to measure the ratios between DIS, QEL and RES neutrino scattering). Additionally, at a Neutrino Factory, where the wrong-sign muon signature is used to measure the golden channel, a measurement of the charm cross-section is needed, since this is the main background to the oscillation signal, and a silicon vertex detector would be able to make this measurement [48]. Other measurements with the near detector include fundamental electroweak parameters (such as $\sin^2\theta_W$) or QCD physics (structure functions, for example). Another important topic for the near detector is the search for Non Standard Interactions (NSI) from a search for taus, either at production or detection [37]. A silicon detector could also carry out this measurement.

Current examples of near detectors at neutrino experiments include the MINOS near detector or the ND280 at T2K [49]. Future neutrino oscillation experiments have developed different near detector concepts. At LBNE, the HiRes near detector concept [50] includes a straw tube transition radiation tracker inside a magnetic field for high resolution track reconstruction and electron-pion separation.

Simulations of a near detector at a Neutrino Factory include the concept of a scintillating fibre tracker inside a magnetic field [51] to measure the neutrino flux through leptonic interactions in the detector, such as Inverse Muon Decay (IMD), with a 11 GeV threshold. An analysis of IMD at a Neutrino Factory near detector shows that a 1% error in the flux estimation can be attained.

At a Neutrino Factory, a near detector sees a line source (from the 600 m long decay straight) and the far detector sees a point source. Figure 4 shows the flux at 100 m and 1 km from the end of the decay straight of a Neutrino Factory storage ring. The far detector spectrum is more similar to the spectrum at 1 km than the spectrum at 100 m, so these differences need to be taken into account in the flux measurement. A matrix method, similar to MINOS, was developed to extrapolate from near to far detectors [52, 53]. By using the spectrum from the near detector to fit the far detector spectrum, the error on the fit improves by 30% at the 3σ level [16].

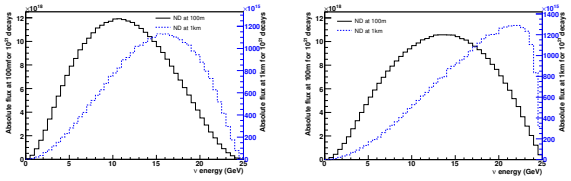

FIGURE 4. (Left) ν_e flux through a 1 m radius detector 100 m and 1 km from a 600 m decay straight of a Neutrino Factory; (right) ν_μ flux for the same detectors (using unpolarised muon expectation).

8. CONCLUSIONS

Two Magnetised Iron Neutrino Detectors (MIND) at 4000 km (with 100 kton mass) and 7500 km (the magic baseline with 50 kton mass), at a Neutrino Factory with 25 GeV/c muons is the default configuration from the International Design Study for a Neutrino Factory (IDS-NF). A new analysis using the NUANCE event generator, a GEANT4 simulation, full pattern recognition and reconstruction improves the detection efficiency at low energies and provides a 3σ discovery of θ_{13}, δ_{CP} and the mass hierarchy down to $\theta_{13} \sim 0.25^o$.

A Totally Active Scintillator Detector (TASD) with lower threshold is especially relevant for a Low Energy Neutrino Factory (LENF) with 5 GeV/c muons. Tau detection, especially in a near detector, has relevance for Non-Standard Interactions. It will be difficult for an emulsion detector to cope with the neutrino interaction rate but a silicon detector would be able to carry out this measurement. Liquid argon detectors are now running routinely and offer possibilities for future larger detectors, but the technology needed to scale the detector size is still ambitious. The next generation of water Cherenkov detectors being considered is in the 100-500 kton scale. While the technology is well understood, the size of these detectors poses significant challenges. Near detectors, especially at a Neutrino Factory, need to have high granularity to be able to measure the neutrino flux and be able to extrapolate to the far detector.

ACKNOWLEDGMENTS

The author acknowledges the support of the Science and Technology Facilities Council, the European Community under the European Commission Framework Programme 7 Design Study: EUROnu, Project Number 212372 and UKIERI for providing travel funds to this workshop.

REFERENCES

1. A. De Rujula, M. B. Gavela, and P. Hernandez, *Nucl. Phys.* **B547**, 21–38 (1999).
2. A. Cervera, et al., *Nucl. Phys.* **B579**, 17–55 (2000).
3. A. Bandyopadhyay, et al., *Rept. Prog. Phys.* **72** (2009).
4. T. Abe, et al., *JINST* **4**, T05001 (2009).
5. The International Design Study for the Neutrino Factory (2010), URL: https://www.ids-nf.org/wiki/FrontPage.
6. EUROnu: A High Intensity Neutrino Oscillation Facility in Europe (2010), URL: http://www.euronu.org/.
7. P. Huber, and W. Winter, *Phys. Rev.* **D68**, 037301 (2003).
8. Geant 3.21 CERN Program Library (1993), CERN Long write up W5013. http://wwwasdoc.web.cern.ch/wwwasdoc/pdfdir/geant.pdf.
9. P. Adamson, et al., *Nucl. Instrum. Meth.* **A556**, 119–133 (2006).
10. D. G. Michael, et al., *Nucl. Instrum. Meth.* **A596**, 190–228 (2008).
11. A. Cervera, A. Laing, J. Martin-Albo, and F. J. P. Soler, *Nucl. Instrum. Meth.* **A624**, 601–614 (2010).
12. A. Cervera-Villanueva, J. J. Gomez-Cadenas, and J. A. Hernando, *Nucl. Instrum. Meth.* **A534**, 180–183 (2004).
13. D. Emeliyanov, I. Gorbounov, and I. Kisel, OTR/ITR-CATS: Tracking Based on Cellular Automaton and Kalman Filter (2001), HERA-B note 01-137, http://www-linux.gsi.de/∼ikisel/reco/HERA-B/cats_main.pdf.
14. I. Abt, D. Emelyanov, I. Gorbunov, and I. Kisel, *Nucl. Instrum. Meth.* **A490**, 546–558 (2002).
15. G. Ingelman, A. Edin, and J. Rathsman, *Computer Physics Communications* **101**, 108–134(27) (1997).
16. A. B. Laing (2010), GLA-THESIS-2010-2216.
17. J. Apostolakis, and D. H. Wright, *AIP Conf. Proc.* **896**, 1–10 (2007).
18. D. Casper, *Nucl. Phys. Proc. Suppl.* **112**, 161–170 (2002).
19. A. Pla-Dalmau, A. D. Bross, V. V. Rykalin, and B. M. Wood, Extruded plastic scintillator for MINERvA (2005), proceedings of 2005 IEEE Nuclear Science Symposium and Medical Imaging Conference, El Conquistador Resort, Puerto Rico, 23-29 Oct 2005.
20. P. Adamson, et al., *Phys. Rev.* **D77**, 072002 (2008).
21. V. Lyubushkin, et al., *Eur. Phys. J.* **C63**, 355–381 (2009).
22. A. A. Aguilar-Arevalo, et al., *Phys. Rev.* **D81**, 092005 (2010).
23. A. Rodriguez, et al., *Phys. Rev.* **D78**, 032003 (2008).
24. D. Indumathi, and N. Sinha, *Phys. Rev.* **D80**, 113012 (2009).
25. A. Donini, J. J. Gómez-Cadenas, and D. Meloni, The τ-contamination of the golden muon sample at the Neutrino Factory (2010), arXiv:1005.2275.
26. C. Andreopoulos, et al., *Nucl. Instrum. Meth.* **A614**, 87–104 (2010).
27. R. Wands, Magnetic field simulations of large iron plates for MIND (2010), private communication.
28. G. Ambrosio, et al. (2001), SLAC-R-591; FERMILAB-TM-2149; http://www.slac.stanford.edu/cgi-wrap/getdoc/slac-r-591.pdf.
29. AIDA: Advanced European Infrastructures for Detectors at Accelerators (2010), URL: https://espace.cern.ch/aida/default.aspx.
30. D. Indumathi, *These proceedings* (2011).
31. A. Bross, et al., *PoS* **NUFACT08**, 043 (2008).
32. A. Bross, M. Ellis, S. Geer, O. Mena, and S. Pascoli, *AIP Conf. Proc.* **981**, 187–189 (2008).
33. A. D. Bross, M. Ellis, S. Geer, O. Mena, and S. Pascoli, *Phys. Rev.* **D77**, 093012 (2008).
34. N. Agafonova, et al., *Phys. Lett.* **B691**, 138–145 (2010).
35. R. Acquafredda, et al., *JINST* **4**, P04018 (2009).
36. D. Autiero, et al., *Eur. Phys. J.* **C33**, 243–260 (2004).
37. D. Meloni, T. Ohlsson, W. Winter, and H. Zhang, *JHEP* **04**, 041 (2010).
38. S. Amerio, et al., *Nucl. Instrum. Meth.* **A527**, 329–410 (2004).
39. B. Rebel, *These proceedings* (2011).
40. H. Chen, et al. (2007), FERMILAB-PROPOSAL-0974.
41. A. A. Aguilar-Arevalo, et al., *Phys. Rev. Lett.* **102**, 101802 (2009).
42. D. Gibin, A. Guglielmi, F. Pietropaolo, C. Rubbia, and P. R. Sala, *Nucl. Phys. Proc. Suppl.* **188**, 355–358 (2009).
43. A. Rubbia, *J. Phys. Conf. Ser.* **171**, 012020 (2009).
44. L. Whitehead, *These proceedings* (2011).
45. M. Aoki, K. Hagiwara, and N. Okamura, *Phys. Lett.* **B554**, 121–132 (2003).
46. F. Dufour, T. Kajita, E. Kearns, and K. Okumura, *Phys. Rev.* **D81**, 093001 (2010).
47. A. de Bellefon, et al. (2006).
48. M. Ellis, and F. J. P. Soler, *Nucl. Instrum. Meth.* **A569**, 127–131 (2006).
49. A. Blondel, *These proceedings* (2011).
50. S. Mishra, *These proceedings* (2011).
51. Y. Karadzhov, *AIP Conf. Proc.* **1222**, 467–470 (2010).
52. A. Laing, and F. J. P. Soler, *AIP Conf. Proc.* **981**, 166–168 (2008).
53. A. Laing, and F. J. P. Soler, *PoS* **NUFACT08**, 129 (2008).